Reliably Counting Atomic Planes of Few-Layer Graphene ($n > 4$)

Yee Kan Koh,[†,§,]* Myung-Ho Bae,[‡] David G. Cahill,[†] and Eric Pop[‡]

[†]Department of Materials Science and Engineering, and Frederick Seitz Materials Research Laboratory, University of Illinois, Urbana, Illinois 61801, United States, [‡]Department of Electrical & Computer Engineering, Micro and Nanotechnology Lab, University of Illinois, Urbana, Illinois 61801, United States, and [§]Department of Mechanical Engineering, National University of Singapore, Singapore

ABSTRACT We demonstrate a reliable technique for counting atomic planes (n) of few-layer graphene (FLG) on SiO_2/Si substrates by Raman spectroscopy. Our approach is based on measuring the ratio of the integrated intensity of the G graphene peak and the optical phonon peak of Si, $I(G)/I(Si)$, and is particularly useful in the range $n > 4$ where few methods exist. We compare our results with atomic force microscopy (AFM) measurements and Fresnel equation calculations. Then, we apply our method to unambiguously identify n of FLG devices on SiO_2 and find that the mobility ($\mu \approx 2000$ cm^2 V^{-1} s^{-1}) is independent of layer thickness for $n > 4$. Our findings suggest that electrical transport in gated FLG devices is dominated by carriers near the FLG/SiO_2 interface and is thus limited by the environment, even for $n > 4$.

KEYWORDS: few-layer graphene · number of graphene layers · Raman spectroscopy · graphene thickness · absorbance of monolayer graphene · field-effect mobility of carriers · electrostatic interlayer screening

Monolayer graphene exhibits unique electrical properties, such as the half-integer quantum Hall effect and quantized electrical conductance, due to confinement of its charge carriers in a two-dimensional honeycomb lattice.[1] The exotic properties of monolayer graphene, however, are not always beneficial for the realization of graphene devices or interconnects, and in many cases, few-layer graphenes (FLGs) have more favorable properties for practical applications. (We define FLG as stacks of a few graphitic layers of sp2-bonded carbon atoms with properties different from graphite.) For example, transverse electric fields in bilayer[2] and few-layer[3] graphene can open band gaps up to ~0.2 eV, which is crucial for the operation of field-effect transistors. In addition, FLG provides a better transparent conductive electrode due to the lower sheet resistance,[4] and is less susceptible to the effects of substrate impurities due to interlayer screening.[5] Thus, knowledge of how electrical,[6,7] thermal,[8,9] and mechanical[10] properties evolve from monolayer graphene to graphite will facilitate the development of graphene devices.

Until now, studies of FLG have been relatively limited, partly due to lack of a convenient and reliable method to count the number of layers n. For $n < 4$, the number of graphene layers is typically determined from the relative intensity,[11] shape,[12,13] and position[14] of the G and 2D peaks of the Raman spectra. These prior Raman-based approaches are especially effective in identifying monolayer graphene[12] but counting of $n > 4$ from an analysis of the G and 2D peaks of graphene remains elusive. The number of graphene layers can also be determined from phase contrast microscopy,[15] or from contrast in the intensity of Rayleigh-scattered light collected using a confocal microscope and a spectrometer.[16,17] The contrast, however, depends on the specifications of the optical elements used in the measurements (e.g., the numerical aperture of the objective lens[16]) and the uniformity of background scattered light. Finally, the number of graphene layers can be determined by atomic force microscopy[14] (AFM) and transmission electron microscopy[12] (TEM), but these approaches are often time-consuming and can be affected by experimental artifacts or surface contamination.[18]

In this paper, we describe a convenient approach based on Raman spectroscopy to count the number of layers n of graphene on SiO_2/Si substrates, up to $n = 10$. We find that the ratios of integrated intensity of the G peak and the first-order optical phonon peak of Si, $I(G)/I(Si)$, are discrete and can be used to count the number of graphene layers. The ratio $I(G)/I(Si)$ increases monotonically and discretely with n due to enhanced absorption and Raman scattering of light by thicker graphenes. We validate our approach by measuring the thickness of selected graphenes using AFM. We then
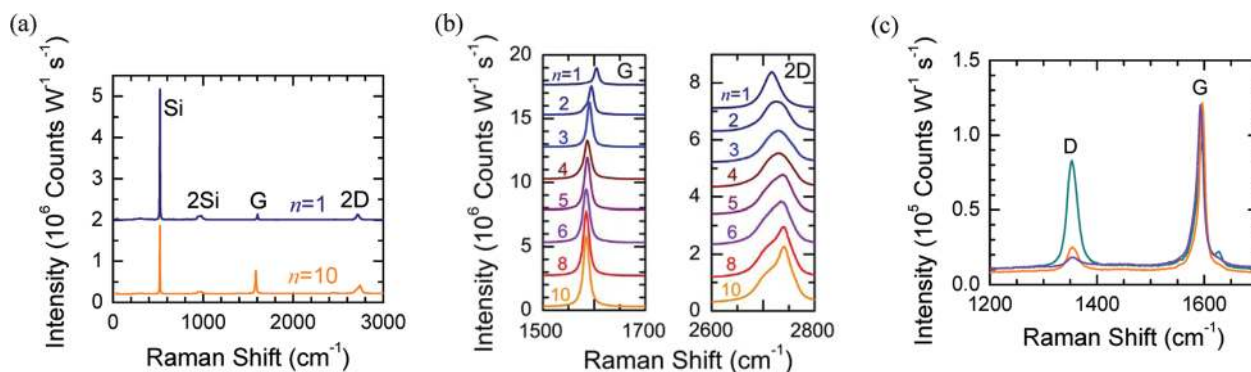
Figure 1. Raman spectra of graphenes on 104 nm SiO₂ on Si substrate. (a) Raman spectra of a monolayer ($n = 1$) and a 10-layer ($n = 10$) graphene. Raman spectrum of the monolayer graphene is up-shifted by 1.0×10^6 counts W^{-1} s^{-1} for clarity. The four most intense peaks are first-order (Si) and second-order (2Si) optical phonon peaks of the silicon substrate, and G peak and 2D peak of graphene. (b) Evolution of intensity and shape of the G and 2D peaks of graphene with the number of layers n. For clarity, multiples of 2.5×10^5 counts W^{-1} s^{-1} and 1.0×10^5 counts W^{-1} s^{-1} are added to the spectra of G and 2D peaks, respectively. (c) Example Raman spectra at three different locations on a graphene flake partially coated with an Au/Ti metal pad. Raman measurements were performed on uncovered regions next to the metal pad. The integrated intensity of G-peak and Si peak (not shown) varies by less than 15% and 1%, respectively, as the integrated intensity of D peaks (indicative of defect level) varies by an order of magnitude.

measure the field-effect mobility of FLGs using patterned four-probe devices, and find $\mu \approx 2000$ cm^2 V^{-1} s^{-1} for $4 \leq n \leq 10$, relatively independent of layer thickness.

RESULTS AND DISCUSSION

There are four pronounced peaks in the Raman spectra[19] of graphene on SiO₂/Si (see Figure 1a). The first two peaks at ~520 cm^{-1} and ~960 cm^{-1} (labeled as "Si" and "2Si") are due to first- and second-order Raman scattering by optical phonons of the Si substrate. The third peak at ~1590 cm^{-1} (the G peak) is due to first-order Raman scattering by doubly degenerate in-plane vibration modes (iTO and LO) at the Brillouin zone center of graphene; while the last peak at ~2740 cm^{-1} (the 2D peak) is due to second-order Raman scattering by in-plane transverse optical phonons (iTO) near the boundary of the Brillouin zone of graphene. As shown in Figure 1a, the intensity of the Si peak and the G peak clearly changes with the number of graphene layers. Although the shape[11–13] and position[14] of the G and 2D peaks also evolves as n increases, see Figure 1b, accurate determination of n for $n > 4$ from the shape and position of the G and 2D peaks is difficult.

An additional Raman peak at ~1350 cm^{-1} (called the D band) appears in graphenes with defects, see Figure 1c. Since the D peak is due to defect-mediated Raman scattering by iTO phonons near the Brillouin zone boundary,[19] the intensity of the D peak is often used as an indicator of the defect density in graphene. The intensity of other peaks could also depend on the defect density in graphene and could therefore limit the usefulness of our counting approach. To study the role of defects on the integrated intensity of the G and Si peaks, we examined monolayer graphene near deposited Au(100 nm)/Ti(2 nm) films; such regions display a significant D peak for reasons that are not known to us. We find that the integrated intensities of the G and Si peaks are relatively insensitive to that of the D peak and thus the defect density in the graphene, see Figure 1c.

We measured the Raman spectra of more than 100 graphene flakes and plot the ratios of integrated intensity of the G and the Si peaks, $I(G)/I(Si)$, in Figure 2. We find that the $I(G)/I(Si)$ ratios for graphenes on 104 nm SiO₂ are fairly discrete for $n = 1-10$ and could be readily used to determine the number of layers of graphene. The ratios of $I(G)/I(Si)$ for graphenes on 280 nm SiO₂, however, are less discrete, especially when $n >$
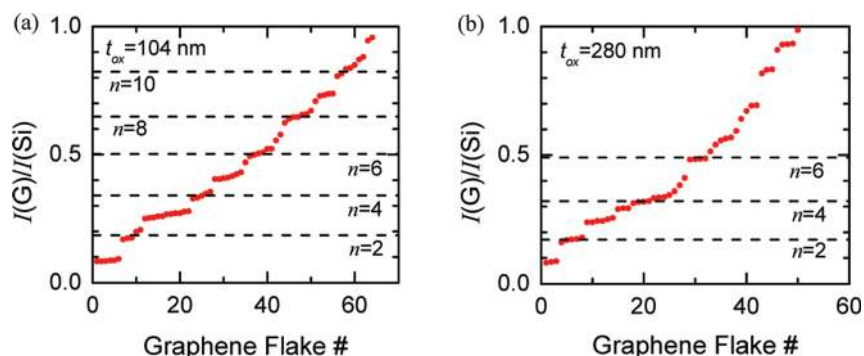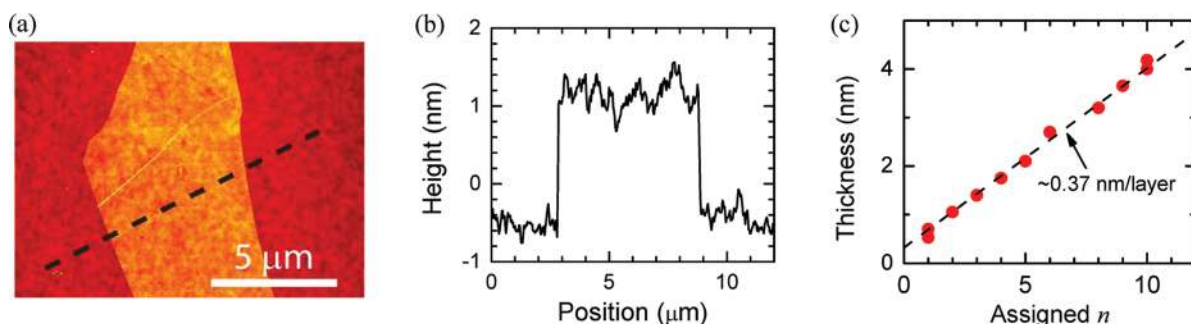

Figure 2. Ratios of the integrated intensity of the G peak, $I(G)$, and the first-order optical phonon peak of silicon, $I(Si)$, for graphene flakes deposited on (a) 104 nm SiO₂ and (b) 280 nm SiO₂ on Si. The graphene flakes are numbered in ascending $I(G)/I(Si)$ order. The dashed lines are the average of the $I(G)/I(Si)$ ratios for the given assigned number of layers n.

Figure 3. Determination of the thickness of selected graphene flakes by atomic force microscopy (AFM): (a) an AFM image of a four-layer graphene; (b) height profile along the dashed line in panel a. The thickness of graphenes is determined from the average of the step heights at the edges of the graphenes. (c) The thickness measured by AFM of selected graphene flakes. The dashed line is a fit to the thickness measurements.

5. We believe that this apparently continuous nature of $I(G)/I(Si)$ is not due to a weak dependence of $I(G)/I(Si)$ on n for graphenes on 280 nm SiO_2, but rather it is because weak color contrast of graphenes on 280 nm SiO_2 during inspection by optical microscopy made regions of homogeneous thickness difficult to identify for the Raman measurements.

In principle, the ratios of the integrated intensity of the 2D and Si peaks, $I(2D)/I(Si)$, could also be discrete, and thus could be used to count n in the same manner as we use $I(G)/I(Si)$. We find, however, that the ratios of $I(2D)/I(Si)$ are nearly continuous (see Figure S1 in the Supporting Information). We attribute this difference in the behavior of $I(G)/I(Si)$ and $I(2D)/I(Si)$ to the fact that the intensity of the 2D peak depends more strongly on carrier density[20] and less strongly on the number of graphitic layers[11] than the intensity of the G peak. Since the carrier density in each individual graphene flake is affected by impurities in and on the graphene flake, $I(2D)/I(Si)$ ratios are not a reliable metric for the number of graphene layers.

We validate n derived from $I(G)/I(Si)$ by measuring the thickness of selected graphene flakes on 104 nm SiO_2 by AFM in a tapping mode, see Figure 3. We determine the thickness from the average step heights at

the graphene edges and plot the thickness of graphene flakes as a function of n assigned from the ratios of $I(G)/I(Si)$ in Figure 3c. The measurements are fit well by a straight line with a slope of ∼0.37 nm per graphene layer, corresponding to the thickness of individual atomic planes in graphite.

We plot the average values of the $I(G)/I(Si)$ ratios as a function of assigned number of graphene layers n in Figure 4a. This data can then be used as a calibration to determine n. We find that $I(G)/I(Si)$ is approximately proportional to n for $1 \leq n \leq 10$, due to an increase of the integrated intensity of the G peak and a decrease of the integrated intensity of the Si peak (see Figure 4b). Since both $I(G)$ and $I(Si)$ are proportional to the power of the incident laser and the efficiency of the collection optics, ratios of $I(G)/I(Si)$ are independent of most experimental parameters and can be used as a reliable method to count n.

In Figure 4, we compare our measurements $I(G)/I(Si)$ to calculations based on the Fresnel equations.[21−23] Details of these calculations are described in the Supporting Information. In the calculations, we assume a four-layered structure consisting of air, graphene, SiO_2, and Si and calculate the transmittances of incident light T_i and of Raman-scattered light T_R. To calculate T_R, we
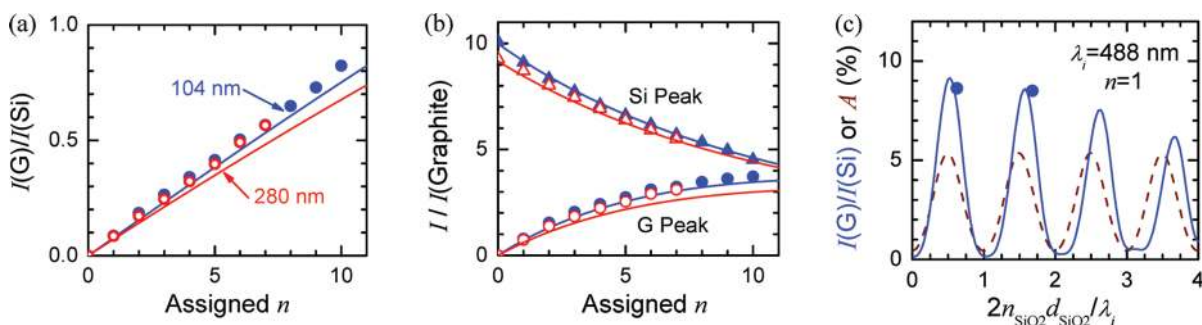
Figure 4. (a) Average values of $I(G)/I(Si)$ of graphenes on 104 nm (blue solid circles) and 280 nm (red open circles) SiO_2 on Si from Figure 2 are plotted as a function of assigned number of layers n of graphene. Solid lines are calculations based on Fresnel equations. (b) Integrated intensity of the first order optical phonon peak of Si (triangles) and the G peak of graphene (circles), normalized by integrated intensity of the G peak of graphite, $I(graphite)$, as a function of assigned n. Solid symbols are measurements of graphenes on 104 nm SiO_2 on Si, while open symbols are measurements of graphenes on 280 nm SiO_2 on Si. The solid lines are, from the top to the bottom, calculations of $I(Si)/I(graphite)$ for graphenes on 104 nm and 280 nm SiO_2 on Si, and calculations of $I(G)/I(graphite)$ for graphenes on 104 nm and 280 nm SiO_2 on Si, respectively. To fit the calculations of $I(Si)/I(graphite)$ to measurements, we assume the ratio of the cross-section for Raman scattering is 1.8 times larger in graphene (or graphite) than in Si. (c) Comparison of calculations of $I(G)/I(Si)$ (solid line) to calculations of the absorbance, A, (dashed line) of monolayer graphene on SiO_2 on Si for $\lambda_i = 488$ nm, as a function of normalized SiO_2 thickness. The solid circles are Raman measurements using $\lambda_i = 488$ nm.
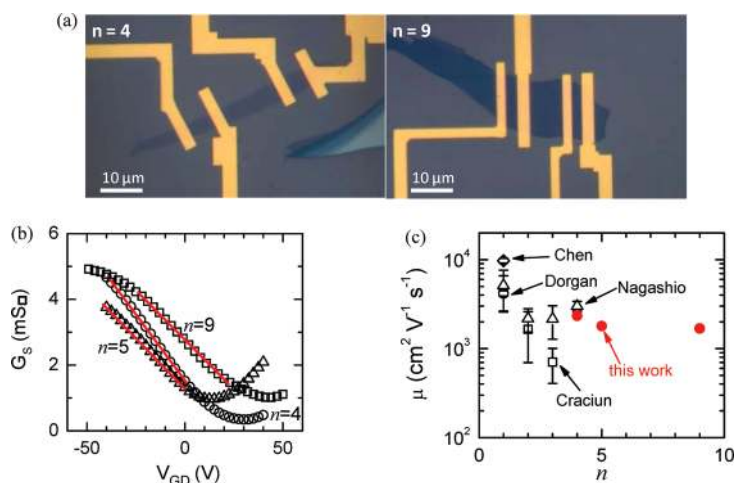
Figure 5. (a) Optical microscope images of the 4-point setup for mobility measurements of graphene flakes with $n = 4$ (left) and $n = 9$ (right). The dimensions (width × length) of the three FLGs are 4.3×15.2 μm^2, 4.1×9.5 μm^2, and 13.4×8.3 μm^2 for $n = 4$, 5, and 9, respectively. **(b)** Sheet conductance of three FLGs as a function of gate voltage. The field-effect mobility of FLGs is derived from the slope (red lines) of the sheet conductance measurements. **(c)** The field-effect mobility of FLGs (solid circles) measured by 4-point setups shown in panel a. Measurements by Chen *et al.* (open diamond, ref 28), Dorgan *et al.* (open circle, ref 26), Craciun *et al.* (open squares, ref 6), and Nagashio *et al.* (open triangles, ref 7) are included for comparison. (The measurements for $n = 1$ by Craciun and Dorgan overlap in the plot.) The error bars indicate the variation of mobility measurements for different graphene samples reported by the same authors and do not represent the full uncertainty of the measurements. Slight variability between the studies is introduced by the approach chosen, that is, Hall mobility (Craciun[6]), effective mobility (Nagashio,[7] Dorgan,[26] and Chen[28]), and field-effect mobility (this work).

assume that Raman-scattered light is random in direction but is sufficiently monochromatic that reflections from interfaces must be treated coherently. We argue that the integrated intensity of the G peak and the Si peak are proportional to T_i, T_R, and the cross-section per unit thickness σ for Raman scattering by the G-band in graphene and the LO phonon of Si, respectively. We assume $\sigma_{graphene} = \sigma_{graphite}$ and derive $\sigma_{graphite} = 1.8\sigma_{Si}$ by fitting the calculations to measurements of $I(Si)/I(Graphite)$ (see Figure 4b). Our calculations agree with our measurements of $I(G)/I(Si)$ (see Figure 4a).

We plot in Figure 4c our calculations of the ratios of $I(G)/I(Si)$ of monolayer graphene on SiO$_2$/Si, and the absorbance A of incident light by the monolayer graphene, as a function of normalized SiO$_2$ thickness. We find that $I(G)/I(Si)$ and A are correlated, suggesting that the observed increase in $I(G)/I(Si)$ with n is mostly due to enhanced absorption[24,25] of light by thicker graphene.

Finally, as a demonstration of the utility of our approach, we fabricated three field-effect transistors (FETs) from FLGs on 104 nm SiO$_2$ on Si, and measured their field-effect mobility, see Figure 5a and Methods for details. We use the Si substrate as the back-gate electrode and monitor the voltage drop across the two inner electrodes under a fixed current bias of $I = 5$ μA. We plot the 4-probe sheet conductance (G_S) as a function of back-gate voltage (V_{GD}) in Figure 5b. The field-effect mobility is then derived from the slope of the plot using

the expression $\mu = (1/C_{ox})(dG_S/dV_{GD})$, where $C_{ox} = 3.3 \times 10^{-4}$ F m^{-2} is the oxide capacitance of the 104 nm thick SiO$_2$ layer. This expression of mobility is only applied to the linear portion of the $G_S - V_{GD}$ curves as shown by the red lines in Figure 5b, because the mobility changes rapidly with carrier density near the Dirac point.[26] We emphasize that our measurements are averages of mobility for charge carriers unevenly distributed between the various layers in the graphene samples; the average mobility is weighted toward the mobility of carriers close to the FLG/SiO$_2$ interface, even for $n > 4$. This is because the electrostatic potential applied by the gate, along with the short screening length[5,27] of ~4 layers, confines the induced carriers within a few atomic layers close to the FLG/SiO$_2$ interface, in a manner similar to the inversion layer of a MOSFET.

We compare the average mobility with measurements by Chen *et al.*,[28] Dorgan et al.,[26] Craciun *et al.*,[6] and Nagashio *et al.*[7] (see Figure 5c). Overall, we find that the mobility of our supported FLG samples is ~2000 cm^2 V^{-1} s^{-1} and only weakly depends on n for $4 \leq n \leq 10$. The weak dependence on n is consistent with our assertion that transport is heavily weighted toward carriers close to the FLG/SiO$_2$ interface due to gating and interlayer screening. Our value for the mobility is an order of magnitude smaller than in graphite,[29] suggesting that the mobility of carriers in FLG on SiO$_2$ could be limited by the environment, such as charged impurities[30] and remote interfacial phonons[26,28] in SiO$_2$, even when $n = 10$. The number of charge impurities electrostatically affecting the graphene device can be estimated from the position of the Dirac voltage $V_0 = 10-45$ V in Figure 5b, that is, an impurity density $C_{ox}V_0/q \approx 2 \times 10^{12}$ to 9×10^{12} cm^{-2}. The positive sign of V_0 indicates p-type doping. One possible source of the unintentional doping is the adsorption of water vapor,[31,32] either from water on the substrate, or through adsorption on the FLG surface.

CONCLUSION

In conclusion, we described a convenient approach for counting the number of layers n of graphenes based on the ratios of the integrated intensity of the G-band Raman peak of graphene and Raman peak of the Si substrate. This new approach is accurate over the range $1 < n < 10$ and could enable significant advances in research of few-layer graphene. We validate our results using AFM measurements and find good agreement

between our data and an optical model of the graphene/SiO$_2$/Si stack. Finally, we apply our approach to identify 4−10 layer graphenes for mobility measurements. Interestingly, we find that the mobility appears independent of layer thickness in this regime, suggesting a strong role of interlayer screening. Our approach should also be compatible for easily counting the number of layers in graphene suspended on a trench or supported on any substrates with Raman-active vibrational modes, for example, PMMA or SiC.[33]

METHODS

We deposited graphene on 104 and 280 nm of SiO$_2$ on highly doped Si by mechanical exfoliation[31] of natural graphite using adhesive tape. We located samples using an optical microscope and annealed them at 400 °C for 35 min in Ar/H$_2$ mixture gas to remove adhesive tape residues from the substrate.[34] We measured spectra of the graphene flakes with a custom-built Raman spectrometer using a laser excitation wavelength of 488 nm and ~1 mW laser power. We use a single 20× objective lens with NA = 0.4 to focus the laser beam and to collect Raman-scattered light in all polarization directions. The Raman spectra are measured using a grating with 1200 g/mm blazed at 500 nm and a solid-state-cooled CCD detector. The full-width-half-maximum spectral resolution of our Raman setup is ~6 cm^{-1}.

To fabricate field-effect transistors based on the few-layer graphenes, we patterned four Au (40 nm)/Ti (2 nm) metal electrodes on each graphene by electron-beam lithography, electron-beam evaporation, and lift-off, as shown in Figure 5a. We used the highly degenerated Si substrate as a back-gate electrode. For the electrical measurements, we used the Keithley 4200 semiconductor characterization system. We monitored the voltage drop across the two inner electrodes under a fixed current bias of $I = 5$ µA through the outer two electrodes as the back-gate voltage is tuned from −40 to 40 V. All electrical measurements were performed at room temperature in a vacuum of ~10^{-5} Torr.

Supporting Information Available: Measurements of the ratios of the integrated intensity of the 2D and Si peaks, a detailed description of the calculations of the intensity of the Si peak and the G peak of Raman spectra of graphene on SiO$_2$ on Si, and the absorption of light by graphene on SiO$_2$ on Si. This material is available free of charge *via* the Internet at http://pubs.acs.org.

REFERENCES AND NOTES

1. Geim, A. K. Graphene: Status and Prospects. *Science* **2009**, *324*, 1530–1534.
2. Castro, E. V.; Novoselov, K. S.; Morozov, S. V.; Peres, N. M. R.; Lopes dos Santos, J. M. B.; Nilsson, J.; Guinea, F.; Geim, A. K.; Castro Neto, A. H. Biased Bilayer Graphene: Semiconductor with a Gap Tunable by the Electric Field Effect. *Phys. Rev. Lett.* **2007**, *99*, 216802.
3. Gava, P.; Lazzeri, M.; Marco Saitta, A.; Mauri, F. Ab Initio Study of Gap Opening and Screening Effects in Gated Bilayer Graphene. *Phys. Rev. B* **2009**, *79*, 165431.
4. Li, X.; Zhu, Y.; Cai, W.; Borysiak, M.; Han, B.; Chen, D.; Piner, R. D.; Colombo, L.; Ruoff, R. S. Transfer of Large-Area Graphene Films for High-Performance Transparent Conductive Electrodes. *Nano Lett.* **2009**, *9*, 4359–4363.
5. Sui, Y.; Appenzeller, J. Screening and Interlayer Coupling in Multilayer Graphene Field-Effect Transistors. *Nano Lett.* **2009**, *9*, 2973–2977.
6. Craciun, M. F.; Russo, S.; Yamamoto, M.; Oostinga, J. B.; Morpurgo, A. F.; Tarucha, S. Trilayer Graphene is a Semimetal with a Gate-Tunable Band Overlap. *Nat. Nanotechnol.* **2009**, *4*, 383–388.
7. Nagashio, K.; Nishimura, T.; Kita, K.; Toriumi, A. Mobility Variations in Mono- and Multilayer Graphene Films. *Appl. Phys. Exp.* **2009**, *2*, 025003.
8. Koh, Y. K.; Bae, M.-H.; Pop, E.; Cahill, D. G. Heat Conduction across Monolayer and Few-Layer Graphenes. *Nano Lett.* **2010**, *10*, 4363.
9. Ghosh, S.; Bao, W.; Nika, D. L.; Subrina, S.; Pokatilov, E. P.; Lau, C. N.; Balandin, A. A. Dimensional Crossover of Thermal Transport in Few-Layer Graphene. *Nat. Mater.* **2010**, *9*, 555–558.
10. Poot, M.; van der Zant, H. S. J. Nanomechanical Properties of Few-Layer Graphene Membranes. *Appl. Phys. Lett.* **2008**, *92*, 063111.
11. Graf, D.; Molitor, F.; Ensslin, K.; Stampfer, C.; Jungen, A.; Hierold, C.; Wirtz, L. Spatially Resolved Raman Spectroscopy of Single- and Few-Layer Graphene. *Nano Lett.* **2007**, *7*, 238–242.
12. Ferrari, A. C.; Meyer, J. C.; Scardaci, V.; Casiraghi, C.; Lazzeri, M.; Mauri, F.; Piscanec, S.; Jiang, D.; Novoselov, K. S.; Roth, S.; *et al.* Raman Spectrum of Graphene and Graphene Layers. *Phys. Rev. Lett.* **2006**, *97*, 187401.
13. Hao, Y.; Wang, Y.; Wang, L.; Ni, Z.; Wang, Z.; Wang, R.; Koo, C. K.; Shen, Z.; Thong, J. T. L. Probing Layer Number and Stacking Order of Few-Layer Graphene by Raman Spectroscopy. *Small* **2010**, *6*, 195–200.
14. Gupta, A.; Chen, G.; Joshi, P.; Tadigadapa, S.; Eklund, P. C. Raman Scattering from High-Frequency Phonons in Supported *n*-Graphene Layer Films. *Nano Lett.* **2006**, *6*, 2667–2673.
15. Wang, Z.; Chun, I. S.; Li, X.; Ong, Z.-Y.; Pop, E.; Millet, L.; Gillette, M.; Popescu, G. Topography and Refractometry of Nanostructures Using Spatial Light Interference Microscopy. *Opt. Lett.* **2010**, *35*, 208.
16. Casiraghi, C.; Hartschuh, A.; Lidorikis, E.; Qian, H.; Harutyunyan, H.; Gokus, T.; Novoselov, K. S.; Ferrari, A. C. Rayleigh Imaging of Graphene and Graphene Layers. *Nano Lett.* **2007**, *7*, 2711–2717.
17. Ni, Z. H.; Wang, H. M.; Kasim, J.; Fan, H. M.; Yu, T.; Wu, Y. H.; Feng, Y. P.; Shen, Z. X. Graphene Thickness Determination Using Reflection and Contrast Spectroscopy. *Nano Lett.* **2009**, *7*, 2758–2763.
18. Nemes-Incze, P.; Osváth, Z.; Kamarás, K.; Biró, L. P. Anomalies in Thickness Measurements of Graphene and Few Layer Graphite Crystals by Tapping Mode Atomic Force Microscopy. *Carbon* **2008**, *46*, 1435–1442.
19. Malard, L. M.; Pimenta, M. A.; Dresselhaus, G.; Dresselhaus, M. S. Raman Spectroscopy in Graphene. *Phys. Rep.* **2009**, *473*, 51–87.
20. Das, A.; Pisana, S.; Chakraborty, B.; Piscanec, S.; Saha, S. K.; Waghmare, U. V.; Novoselov, K. S.; Krishnamurthy, H. R.; Geim, A. K.; Ferrari, A. C.; *et al.* Monitoring Dopants by Raman Scattering in an Electrochemically Top-Gated Graphene Transistor. *Nat. Nanotechnol.* **2008**, *3*, 210.
21. Blake, P.; Hill, E. W.; Castro Neto, A. H.; Novoselov, K. S.; Jiang, D.; Yang, R.; Booth, T. J.; Geim, A. K. Making Graphene Visible. *Appl. Phys. Lett.* **2007**, *91*, 063124.
22. Wang, Y. Y.; Ni, Z. H.; Shan, Z. X.; Wang, H. M.; Wu, Y. H. Interference Enhancement of Raman Signal of Graphene. *Appl. Phys. Lett.* **2008**, *92*, 043121.
23. Yoon, D.; Moon, H.; Son, Y.-W.; Choi, J. S.; Park, B. H.; Cha,

Y. H.; Kim, Y. D.; Cheong, H. Interference Effect on Raman Spectrum of Graphene on SiO$_2$/Si. *Phys. Rev. B* **2009**, *80*, 125422.

24. Nair, R. R.; Blake, P.; Grigorenko, A. N.; Novoselov, K. S.; Booth, T. J.; Stauber, T.; Peres, N. M. R.; Geim, A. K. Fine Structure Constant Defines Visual Transparency of Graphene. *Science* **2008**, *320*, 1308.

25. Mak, K. F.; Sfeir, M. Y.; Wu, Y.; Lui, C. H.; Misewich, J. A.; Heinz, T. F. Measurement of the Optical Conductivity of Graphene. *Phys. Rev. Lett.* **2008**, *101*, 196405.

26. Dorgan, V. E.; Bae, M.-H.; Pop, E. Mobility and Saturation Velocity in Graphene on SiO$_2$. *Appl. Phys. Lett.* **2010**, *97*, 082112.

27. Miyazaki, H.; Odaka, S.; Sato, T.; Tanaka, S.; Goto, H.; Kanda, A.; Tsukagoshi, K.; Ootuka, Y.; Aoyagi, Y. Interlayer Screening Length to Electric Field in Thin Graphite Film. *Appl. Phys. Express* **2008**, *1*, 034007.

28. Chen, J.-H.; Jang, C.; Xiao, S.; Ishigami, M.; Fuhrer, M. S. Instrinsic and Extrinsic Performance Limits of Graphene Devices on SiO$_2$. *Nat. Nanotechnol.* **2008**, *3*, 206–209.

29. Sugihara, K.; Kawamura, K.; Tsuzuku, T. Temperature Dependence of the Average Mobility in Graphite. *J. Phys. Soc. Jpn.* **1979**, *47*, 1210–1215.

30. Tan, Y.-W.; Zhang, Y.; Bolotin, K.; Zhao, Y.; Adam, S.; Hwang, E. H.; Das Sarma, S.; Stormer, H. L.; Kim, P. Measurement of Scattering Rate and Minimum Conductivity in Graphene. *Phys. Rev. Lett.* **2007**, *99*, 246803.

31. Novoselov, K. S.; Geim, A. K.; Morozov, S. V.; Jiang, D.; Zhang, Y.; Dubonos, S. V.; Grigorieva, I. V.; Firsov, A. A. Electric Field Effect in Atomically Thin Carbon Films. *Science* **2004**, *306*, 666.

32. Leenaerts, O.; Partoens, B.; Peeters, F. M. Adsorption of H$_2$O, NH$_3$, CO, NO$_2$ on Graphene: A First-Principles Study. *Phys. Rev. B* **2008**, *77*, 125416.

33. Shivaraman, S.; Chandrashekhar, M. V. S.; Boeckl, J. J.; Spencer, M. G. Thickness Estimation of Epitaxial Graphene on SiC Using Attenuation of Substrate Raman Intensity. *J. Electr. Mater.* **2009**, *38*, 725–730.

34. Ishigami, M.; Chen, J. H.; Cullen, W. G.; Fuhrer, M. S.; Williams, E. D. Atomic Structure of Graphene on SiO$_2$. *Nano Lett.* **2007**, *7*, 1643–1648.